# Electron-impact single ionization of Mg and $Al^+$

J. A. Ludlow, C. P. Ballance, S. D. Loch, and M. S. Pindzola
*Department of Physics, Auburn University, Auburn, Alabama, 36849 USA*

D. C. Griffin
*Department of Physics, Rollins College, Winter Park, Florida, 32789 USA*

(Received 20 January 2009; published 31 March 2009)

Theory and experiment are compared for the electron-impact single ionization of Mg and $Al^+$. Nonperturbative *R* matrix with pseudostates (RMPS) and time-dependent close-coupling (TDCC) calculations have been carried out that exhibit large reductions from perturbative distorted-wave results of 38% for Mg and 20% for $Al^+$. Experimental single-ionization data available for Mg and $Al^+$ are in reasonable accord with distorted-wave data and lie substantially above the new theoretical results. Rate coefficients, necessary for the collisional-radiative modeling of Mg and Al plasmas were generated from the RMPS ionization cross sections. In the collisional-ionization region near the ionization threshold, the resulting rates were found to be up to two times lower for Mg and three times lower for $Al^+$ than the rates generated from experimental data.

DOI: 10.1103/PhysRevA.79.032715 PACS number(s): 34.80.Dp

## I. INTRODUCTION

Electron-impact ionization of atoms and ions has been of continuing interest for many decades due to its importance in areas such as controlled fusion plasmas [1] and astrophysics [2]. For atomic ions that are more than a few times ionized, perturbative distorted-wave methods have been found to give accurate results for ground-state ionization. However, for neutral and near-neutral systems, perturbative methods consistently overestimate the cross section close to the ionization peak and it becomes necessary to employ nonperturbative methods to properly account for the long-range Coulomb interaction between the ejected and scattered electrons. This has spurred the development of nonperturbative theories such as time-dependent close coupling (TDCC) [3], *R*–matrix with pseudostates (RMPSs) [4], and convergent close coupling (CCC) [5]. Agreement between nonperturbative theory and experiment for electron-impact ionization of ground-state neutrals and near neutrals has been mixed across the Periodic Table.

For the ground state of noble gases, theory and experiment are in good accord. For He ($1s^2$), CCC [6], RMPS [7], and TDCC [8] calculations are in excellent agreement with experiment [9]. For Ne ($1s^22s^22p^6$), an RMPS calculation is currently in progress, but preliminary calculations exhibit good agreement with experiment. The TDCC method overestimates the cross section [10] for neon when compared to experiment [11] due to the neglect of term dependence in the ejected-electron continuum. For Ar ($1s^22s^22p^63s^23p^6$), a recent RMPS calculation has been performed [4] and was found to be in good agreement with experiment [12,13].

In the case of systems with one valence electron, experiment and theory are often at odds. Starting with lithiumlike systems ($1s^22s$), in the case of Li, nonperturbative RMPS, TDCC, and CCC calculations agree well with each other [14] but lie well below experiment [15]. A similar trend is seen for $Be^+$, where again the TDCC and RMPS [16,17] results along with a CCC calculation [18] are in good agreement with each other but fall substantially below experiment [19]. For $B^{2+}$, experiment [20] and theory [20,21] are in good agreement. Furthermore, for sodiumlike systems ($1s^22s^23s$), a CCC calculation [22] for neutral Na, which initially disagreed with existing experimental data, prompted a new experimental measurement [23] to address the discrepancy. Similarly for $Al^{2+}$, nonperturbative theory [24] disagreed with existing experimental data [25], prompting a new experiment [26] to investigate the difference. Yet for $Mg^+$, TDCC, RMPS, and CCC results agree well with each other [24] and experiment [27].

Nonperturbative calculations for berylliumlike systems ($1s^22s^2$) include TDCC and RMPS studies for Be [17], $B^+$, [28] and $C^{2+}$ [29]. In addition a recent TDCC calculation for magnesiumlike ($1s^22s^22p^63s^2$) $Si^{2+}$ [30] has been performed. For these systems, distorted-wave methods were found to overestimate the peak of the ionization cross section, with nonperturbative calculations lying 38% below distorted-wave values for Be, 14% for $B^+$, 20% for $C^{2+}$, and 11% for $Si^{2+}$. Experiments for $B^+$ [28], $C^{2+}$ [29], and $Si^{2+}$ [31] appear to have problems with metastable contamination in the ion beam. For $B^+$, an experimentally determined metastable fraction of 9% gave good agreement with theory. For $C^{2+}$, an assumed metastable fraction of 60% resulted in reasonable agreement with theory. In the case of $Si^{2+}$, the metastable fraction was unknown, which complicates comparison with theory.

The most recent experimental data available for both Mg [32,33] and $Al^+$ [34–36] show reasonable agreement with distorted-wave calculations. Taking into consideration the poor performance of distorted-wave calculations for other near-neutral two valence-electron systems, this agreement is surprising. In addition, experimental data for near neutrals, where nonperturbative theoretical results are available, have been seen to be of varying quality. To help assess the accuracy of the existing experimental data, we decided to study the electron-impact ionization of ground-state Mg and $Al^+$ using the TDCC and RMPS methods. Therefore, the electron-impact ionization of the 3*s* subshell of the $1s^22s^22p^63s^2$ ground configuration for both Mg and $Al^+$ has been calculated below the threshold for 2*p* excitation-autoionization.

 

The rest of the paper is structured as follows. In Sec. II, we provide an overview of the theoretical methods; in Sec. III, the theoretical ionization cross sections and rate coefficients for Mg and $Al^+$ are presented and compared to existing experimental data; and in Sec. IV, we conclude with a brief summary. Unless otherwise stated, we will use atomic units.

## II. THEORETICAL METHODS

### A. Time-dependent close-coupling method

The time-dependent close-coupling method [3] uses a coupled-channel representation of the time-dependent wave function to solve the scattering problem of a particle incident upon a few-body system. Expanding the total wave function in coupled spherical harmonics yields a set of coupled partial differential equations for each *LS* symmetry,

$$i\frac{\partial P^{LS}_{l_1l_2}(r_1,r_2,t)}{\partial t} = T_{l_1l_2}(r_1,r_2)P^{LS}_{l_1l_2}(r_1,r_2,t) + \sum_{l_1',l_2'} U^{L}_{l_1l_2,l_1'l_2'}(r_1,r_2)P^{LS}_{l_1'l_2'}(r_1,r_2,t). \quad (1)$$

Expressions for the kinetic-energy and potential-energy terms can be found in Ref. [10]. The time-dependent close-coupled equations are solved by propagating the equations on a two-dimensional lattice and collision probabilities extracted at a time $t=T$ after the collision. The initial condition for the TDCC solution is given by a product of the $3s$ bound orbital and a Gaussian radial-wave packet. Parity conservation acts as a constraint on the possible $l_1l_2$ channels with $(-1)^{l_1+l_2}=(-1)^{l+l_g}$, where $l$ is the angular momentum of the target subshell and $l_g$ is the angular momentum of the incident Gaussian radial-wave packet. The long-range Coulomb interaction between the ejected and scattered electrons is fully accounted for by this method. The ionization cross section is found via a projection of the radial-wave function $P^{LS}_{l_1l_2}(r_1,r_2,t)$ onto bound radial orbitals in order to extract the partial-scattering probabilities.

In order to avoid the possibility of de-excitation to closed inner subshells during the time propagation [37], it is necessary to construct pseudo-orbitals for the target $3s$ subshell and orbitals needed for projections. The procedure involves first diagonalizing the following radial Hamiltonian for $Mg^+$ and $Al^{2+}$:

$$H(r) = -\frac{1}{2}\frac{\partial^2}{\partial r^2} - \frac{Z}{r} + \frac{l(l+1)}{2r^2} + V^l_{PP}(r), \quad (2)$$

where $Z$ is the nuclear charge and $V^l_{PP}(r)$ is a pseudopotential for the inner $1s^22s^22p^6$ core. We used the pseudopotentials generated by Wadt and Hay [38] for the inner cores of $Mg^+$ and $Al^{2+}$. Then the $Mg^+$ and $Al^{2+}$ pseudo-orbitals resulting from the diagonalization are used to construct direct and exchange potentials for the $3s$ subshell of Mg and $Al^+$. Adding these potentials to the Hamiltonian gives,

$$H(r) = -\frac{1}{2}\frac{\partial^2}{\partial r^2} - \frac{Z}{r} + \frac{l(l+1)}{2r^2} + V^l_{PP}(r) + J^0_{3s} - \frac{\alpha_l}{2}\left(\frac{24\rho_{3s}}{\pi}\right)^{1/3}, \quad (3)$$

where $J^0_{3s}$ is the direct potential and $\rho_{3s}$ is the probability density in the local exchange potential. Diagonalizing with a value of $\alpha=0.4$ gave reasonable eigenenergies for the $3s$ subshells of $-7.81$ eV for Mg and $-19.20$ eV for $Al^+$. This compares to experimental energies of $-7.65$ and $-18.83$ eV, respectively [39].

The TDCC calculations were carried out for all *LS* symmetries from $L=0$ to $L=7$. The number of coupled channels per *LS* symmetry ranged from 9 for $L=0$ to 28 for $L=7$ for Mg and up 36 channels for $L=7$ for $Al^+$. For both Mg and $Al^+$, we employed a $384\times384$ point radial lattice with a uniform mesh spacing of $\Delta r=0.20$. Since good agreement was found between the TDCC and distorted-wave partial cross sections for $l=7$, distorted-wave calculations for $l=8$ to $l=50$ were used to "top up" the low-$l$ TDCC results. Convergence checks were made for Mg at 15 eV using a $512\times512$ point radial lattice, with a uniform mesh spacing of $\Delta r=0.20$. The exchange parameter was varied to $\alpha=0.358$ to give the experimental $3s$ energy of $-7.65$ eV. No significant difference was found with the results obtained from the $384\times384$ lattice.

### B. *R*-matrix with pseudostates method

The RMPS method is an extension of standard *R*-matrix theory that employs pseudostates to represent the high-Rydberg states and the target continuum [40]. Inside the *R*-matrix box, the total wave function for a given $LS\Pi$ symmetry is expanded in basis states given by

$$\Psi^{N+1}_k = A\sum_{i,j} a_{ijk}\psi^{N+1}_i\frac{u_{ij}(r_{N+1})}{r_{N+1}} + \sum_i b_{ik}\chi^{N+1}_i, \quad (4)$$

where $A$ is an antisymmetrization operator, $\psi^{N+1}_i$ are channel functions, $u_{ij}(r)$ are radial continuum basis functions, and $\chi^{N+1}_i$ are $(N+1)$-electron bound wave functions, required for completeness. The coefficients $a_{ijk}$ and $b_{ik}$ are determined by direct diagonalization of the total $(N+1)$-electron Hamiltonian. Outside the *R*-matrix box, the total wave function for a given $LS\Pi$ symmetry is expanded in basis states given by

$$\Psi^{N+1}_k = \sum_i \psi^{N+1}_i\frac{v_i(r_{N+1})}{r_{N+1}}, \quad (5)$$

where $v_i(r)$ are radial continuum functions obtained by solution of radial asymptotic coupled differential equations.

The radial orbitals for the spectroscopic and pseudostates were determined using the atomic structure code AUTOSTRUCTURE [41]. Due to the large number of orbitals and configurations involved, we employed the graphical AUTOSTRUCTURE package (GASP) [42], a java front end to AUTOSTRUCTURE. The spectroscopic orbitals included the $1s-5g$ subshells, calculated with a local potential that was determined using Slater-type orbitals. The higher-Rydberg states and the target continuum were represented using nonorthogonal Laguerre pseudo-orbitals for all subshells from

$6s-14g$. They were subsequently orthogonalized to the spectroscopic orbitals and to each other.

Both Mg and $Al^+$ models use a single $3snl$ pseudostate expansion outside the closed-shell neon core, with the additional $3p^2$, $3p3d$, and $3d^2$ configurations used to improve the $N$-electron structure. These configurations give rise to 127 $LS\Pi$ terms, all of which were included in our close-coupling expansion. In our implementation of the RMPS method, the basis used to represent the $(N+1)$-electron continuum was made orthogonal to the pseudo-orbitals using a method developed by Gorczyca and Badnell [43]. The scattering calculation was performed with our set of parallel $R$-matrix programs [44–47], which are extensively modified versions of the serial RMATRIX I programs [48]. The $R$-matrix box for neutral Mg was approximately 105 a.u., whereas for singly ionized Al this was greatly reduced to approximately 52 a.u. For the total ionization cross-section calculations, we calculated partial waves from $L=0$ to $L=13$ in the energy range from the first ionization threshold to just over 40 eV in the case of Mg and 60 eV for $Al^+$. The contributions from higher partial waves above $L=13$ were then estimated for dipole transitions using the method originally described by Burgess [49] and for nondipole transitions assuming a geometric series in $L$, using energy ratios, with special procedures for handling transitions between nearly degenerate terms. The total ground-state ionization cross sections are determined from the sum of all excitation cross sections from the ground term to those pseudostate terms above the ionization threshold. The cross sections were fitted using two different fitting formulas. From threshold to twice the ionization potential a Rost and Pattard expression [50] was used. This ensured the right threshold behavior for the cross-section fit. For energies higher than twice the ionization potential the expression of Younger [51] was used. A Bethe limit point was generated using a configuration-average distorted-wave code and used in the Younger fit, so that the cross section could be extended to higher energies. A good fit to the raw RMPS data was achieved for both Mg and $Al^+$, with errors typically less than 5% in the near threshold region and less than 2% for the Younger fit.

### C. Distorted-wave method

The configuration-average distorted-wave method is a perturbative method that can be used to calculate total cross sections for electron-impact excitation, ionization, and recombination of atoms and their ions [52]. Contributions to the direct ionization cross section are made by the transitions as follows:

$$(nl)^w k_i l_i \rightarrow (nl)^{w-1} k_e l_e k_f l_f, \tag{6}$$

where $w$ is a subshell occupation number and $k_i l_i$, $k_e l_e$, and $k_f l_f$ are quantum numbers for the incident, ejected, and final continuum electrons, respectively. The configuration-average ionization cross section is given by

$$\sigma_{\text{ion}} = \frac{32w}{k_i^3} \int_0^{E/2} \frac{d(k_e^2/2)}{k_e k_f} \sum_{l_i,l_e,l_f} (2l_i+1)(2l_e+1)(2l_f+1) \times P(nlk_i l_i \rightarrow k_e l_e k_f l_f), \tag{7}$$

where $E=k_e^2/2+k_f^2/2$ and $P$ is the first-order perturbation-theory scattering probability.

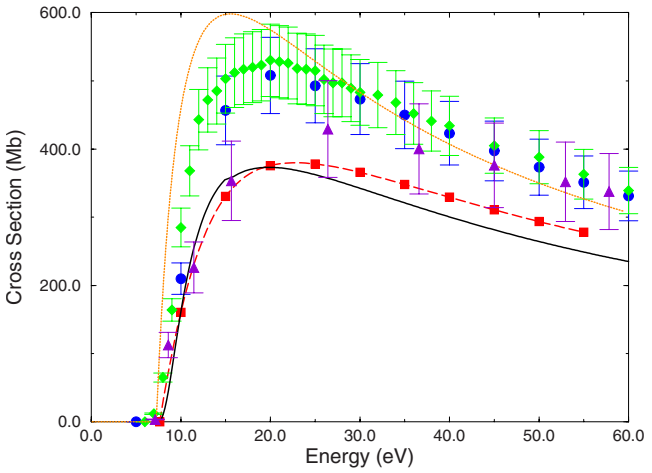


FIG. 1. (Color online) Electron-impact ionization cross section for Mg. Dotted curve: distorted-wave, solid squares: TDCC, solid curve: RMPS, solid circles: experiment [32], solid diamonds: experiment [33], and solid triangles: experiment [60] (1.0 Mb $=1.0\times10^{-18}$ $cm^2$).

The bound radial orbitals for Mg and $Al^+$ were calculated using Cowan's Hartree-Fock (HF) atomic structure code [53]. For direct ionization of the $3s$ subshell of Mg and $Al^+$, we included $l_i=0-50$, $l_e=0-8$, and $l_f=0-50$ in the partial-wave sums in Eq. (7).

## III. RESULTS

Theoretical ionization cross sections for Mg have been reported by Peach [54] and McGuire [55] using variants of the Born approximation, and Jha and Roy [56] have carried out a binary-encounter model calculation. Experimentally, there has been a wide variation in the absolute value of the

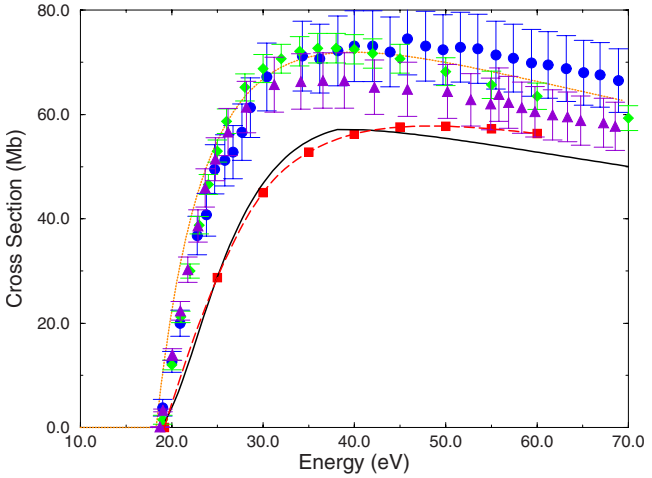


FIG. 2. (Color online) Electron-impact ionization cross section for $Al^+$. Dotted curve: distorted-wave, solid squares: TDCC, solid curve: RMPS, solid circles: experiment [35], solid diamonds: experiment [34], and solid triangles: experiment [36] (1.0 Mb=1.0 $\times10^{-18}$ $cm^2$).

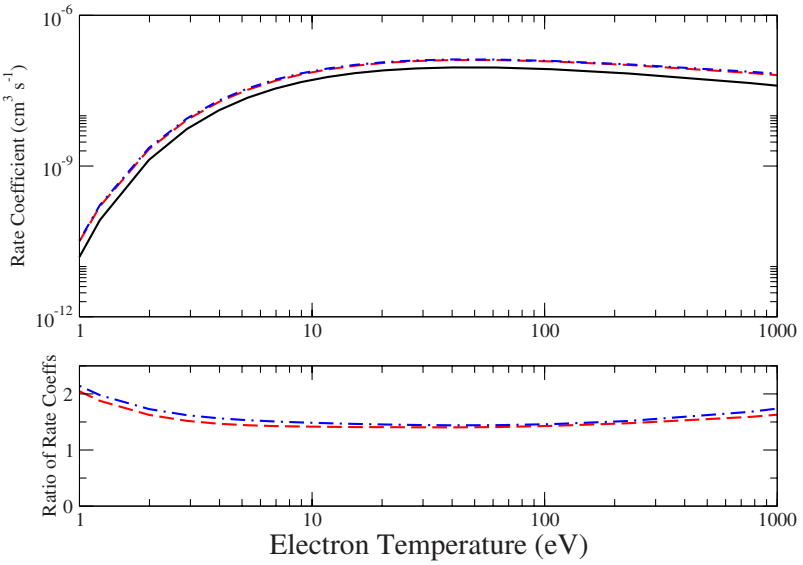


FIG. 3. (Color online) Upper graph: rate coefficients for Mg. Solid curve: RMPS, long-dashed curve: Dere [64], and dotted-dashed curve: Mattioli *et al.* [65]. Lower graph: ratio of other rate coefficients to RMPS rate coefficients. Long-dashed curve: Dere [64] and dotted-dashed curve: Mattioli *et al.* [65].

reported cross sections. Experiments by Karstensen and Schneider [57], Okudaira *et al.* [58], and Okuno *et al.* [59] lie substantially above more recent experiments by Boivin and Srivastava [32] and Freund *et al.* [33] who are in reasonable agreement with perturbative theories. Vainshtein *et al.* [60] measured an ionization cross section that was below any of the other experiments and theoretical results. An experiment by McCallion *et al.* [61] normalized their cross section to the data of Freund *et al.* [33] and so will not be considered here.

Electron-impact ionization cross sections for Mg are presented in Fig. 1. The nonperturbative TDCC and RMPS results are in good agreement with each other. The RMPS results lie about 38% below the peak of the distorted-wave cross section. This behavior is very similar to that observed for Be [17]. The distorted-wave cross section is in reasonable agreement with the previous theoretical calculations by Peach [54] and McGuire [55]. The peak of the nonperturbative RMPS results is 27% lower than the experiment of Boivin [32], 30% lower than Freund *et al.* [33], and 13% lower than Vainshtein *et al.* [60].

Previous theoretical work for the direct ionization of $Al^+$ has been confined to the scaled Born work of McGuire [62] and distorted-wave calculations by Tayal and Henry [63], who also carried out *R*-matrix calculations for excitation-autoionization. The three sets of experimental data we could find for $Al^+$ were those measured by Montague and Harrison [34], Belic *et al.* [35], and Hayton and Peart [36]. The experimental results of Montague and Harrison and Belic *et al.* are in good agreement with each other around the peak of the cross section, both peaking slightly higher than distorted wave, with the results of Hayton and Peart peaking slightly lower than distorted wave. Electron-impact ionization cross sections for $Al^+$ are presented in Fig. 2. The RMPS and TDCC results are in good agreement with each other, lying about 20% below distorted-wave data at the peak. The TDCC results are higher than the RMPS data at larger energies. Previous perturbative calculations by McGuire [62] and Tayal and Henry [63], in reasonable agreement with the present distorted-wave results, overestimate the cross section in comparison to the nonperturbative results.

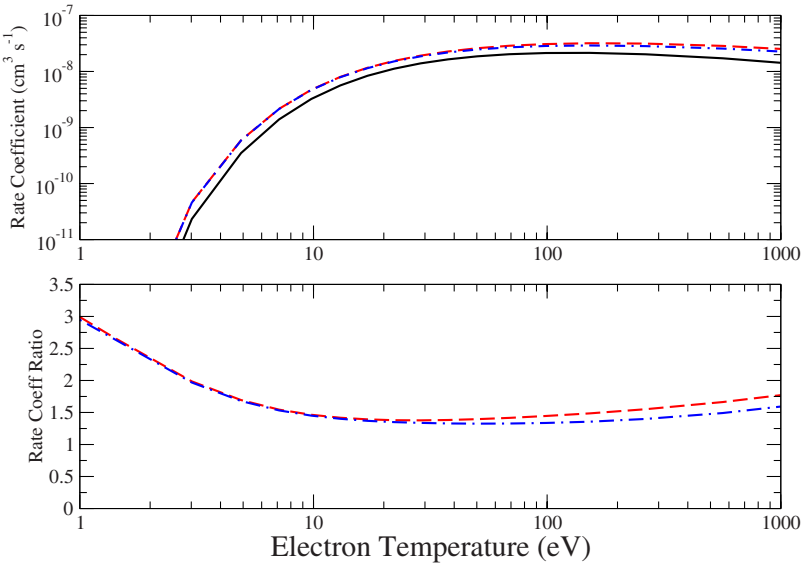


FIG. 4. (Color online) Upper graph: rate coefficients for $Al^+$. Solid curve: RMPS, long-dashed curve: Dere [64], and dotted-dashed curve: Mattioli *et al.* [65]. Lower graph: ratio of other rate coefficients to RMPS rate coefficients. Long-dashed curve: Dere [64] and dotted-dashed curve: Mattioli *et al.* [65].

The present results for Mg and $Al^+$ are consistent with trends observed in the Be sequence [17] and are not unexpected. The existing experimental data for both Mg and $Al^+$ should be reassessed in the light of the present nonperturbative calculations.

Rate coefficients were determined from the fitted RMPS cross-section data. The cross-section fits were convolved with Maxwellian free-electron distributions to make rate coefficients. The results can be seen in Fig. 3 for Mg and in Fig. 4 for $Al^+$ and are compared with the data of Dere [64] and Mattioli *et al.* [65]. For both Mg and $Al^+$, Dere and Mattioli *et al.* use fits to the experimentally measured cross sections. Our rate coefficients are up to a factor of 2 smaller than both of these data sets near the ionization threshold. This is due to the factor-of-2 difference in the ionization cross sections in the near threshold region. By 10 eV our rate coefficients are a factor of 1.4 smaller than the Dere and Mattioli *et al.* data due to differences near the peak of the cross section. This difference persists up to 1000 eV. For $Al^+$ we see similar differences between our RMPS rate coefficients and the data of Dere [64] and Mattioli *et al.* [65]. At low temperatures, our rate coefficients are up to a factor of 3 smaller and by 10 eV the difference is about a factor of 1.5, again due to differences in the underlying cross section.

## IV. SUMMARY

Electron-impact ionization cross sections for Mg and $Al^+$ have been calculated using the nonperturbative TDCC and RMPS methods and the perturbative distorted-wave method. For Mg, the nonperturbative calculations were 38%, and for $Al^+$, 20% below distorted-wave results, showing the importance of properly accounting for the long-range Coulomb interaction. Existing experimental data, in reasonable accord with perturbative distorted-wave theory, are found to strongly overestimate the cross section. Maxwellian-averaged ionization rates based on experimental data are up to two times larger for Mg and three times larger for $Al^+$ in the collisional ionization region near the ionization threshold than rates generated using the nonperturbative ionization cross sections. This should encourage renewed experimental efforts to help to resolve these discrepancies.

## ACKNOWLEDGMENTS

This work was supported in part by grants from the U.S. Department of Energy. Computational work was carried out at the National Energy Research Scientific Computing Center in Oakland, California.

[1] H. Bolt, V. Barabash, G. Federici, J. Linke, A. Loarte, J. Roth, and K. Sato, J. Nucl. Mater. **307–311**, 43 (2002).
[2] T. R. Kallman and P. Palmeri, Rev. Mod. Phys. **79**, 79 (2007).
[3] M. S. Pindzola, F. Robicheaux, S. D. Loch, J. C. Berengut, T. Topcu, J. Colgan, M. Foster, D. C. Griffin, C. P. Ballance, D. R. Schultz, T. Minami, N. R. Badnell, M. C. Witthoeft, D. R. Plante, D. M. Mitnik, J. A. Ludlow, and U. Kleiman, J. Phys. B **40**, R39 (2007).
[4] C. P. Ballance, D. C. Griffin, M. S. Pindzola, and S. D. Loch, J. Phys. B **40**, F27 (2007).
[5] I. Bray, Phys. Rev. Lett. **89**, 273201 (2002).
[6] D. V. Fursa and I. Bray, Phys. Rev. A **52**, 1279 (1995).
[7] E. T. Hudson, K. Bartschat, M. P. Scott, P. G. Burke, and V. M. Burke, J. Phys. B **29**, 5513 (1996).
[8] M. S. Pindzola, D. M. Mitnik, J. Colgan, and D. C. Griffin, Phys. Rev. A **61**, 052712 (2000).
[9] R. K. Montague, M. F. A. Harrison, and A. C. H. Smith, J. Phys. B **17**, 3295 (1984).
[10] M. S. Pindzola, J. Colgan, F. Robicheaux, and D. C. Griffin, Phys. Rev. A **62**, 042705 (2000).
[11] E. Krishnakumar and S. K. Srivastava, J. Phys. B **21**, 1055 (1988).
[12] R. C. Wetzel, F. A. Baiocchi, T. R. Hayes, and R. S. Freund, Phys. Rev. A **35**, 559 (1987).
[13] H. C. Straub, P. Renault, B. G. Lindsay, K. A. Smith, and R. F. Stebbings, Phys. Rev. A **52**, 1115 (1995).
[14] J. Colgan, M. S. Pindzola, D. M. Mitnik, D. C. Griffin, and I. Bray, Phys. Rev. Lett. **87**, 213201 (2001).
[15] I. P. Zapesochnyi and I. S. Aleksakhin, Zh. Eksp. Teor. Fiz. **55**, 76 (1968) [Sov. Phys. JETP **28**, 41 (1969)].
[16] M. S. Pindzola, F. Robicheaux, N. R. Badnell, and T. W. Gorczyca, Phys. Rev. A **56**, 1994 (1997).
[17] J. Colgan, S. D. Loch, M. S. Pindzola, C. P. Ballance, and D. C. Griffin, Phys. Rev. A **68**, 032712 (2003).
[18] K. Bartschat and I. Bray, J. Phys. B **30**, L109 (1997).
[19] R. A. Falk and G. H. Dunn, Phys. Rev. A **27**, 754 (1983).
[20] O. Woitke, N. Djuric, G. H. Dunn, M. E. Bannister, A. C. H. Smith, B. Wallbank, N. R. Badnell, and M. S. Pindzola, Phys. Rev. A **58**, 4512 (1998).
[21] P. J. Marchalant, K. Bartschat, and I. Bray, J. Phys. B **30**, L435 (1997).
[22] I. Bray, Phys. Rev. Lett. **73**, 1088 (1994).
[23] A. R. Johnston and P. D. Burrow, Phys. Rev. A **51**, R1735 (1995).
[24] N. R. Badnell, M. S. Pindzola, I. Bray, and D. C. Griffin, J. Phys. B **31**, 911 (1998).
[25] D. H. Crandall, R. A. Phaneuf, R. A. Falk, D. S. Belic, and G. H. Dunn, Phys. Rev. A **25**, 143 (1982).
[26] J. W. G. Thomason and B. Peart, J. Phys. B **31**, L201 (1998).
[27] B. Peart, J. W. G. Thomason, and K. Dolder, J. Phys. B **24**, 4453 (1991).
[28] J. C. Berengut, S. D. Loch, M. S. Pindzola, C. P. Ballance, D. C. Griffin, M. Fogle, and M. E. Bannister, Phys. Rev. A **78**, 012704 (2008).
[29] S. D. Loch, M. C. Witthoeft, M. S. Pindzola, I. Bray, D. V. Fursa, M. Fogle, R. Schuch, P. Glans, C. P. Ballance, and D. C. Griffin, Phys. Rev. A **71**, 012716 (2005).
[30] J. Colgan, H. L. Zhang, and C. J. Fontes, Phys. Rev. A **77**, 062704 (2008).
[31] N. J. Djurić, E. W. Bell, X. Q. Guo, G. H. Dunn, R. A. Phaneuf, M. E. Bannister, M. S. Pindzola, and D. C. Griffin, Phys. Rev. A **47**, 4786 (1993).

[32] R. F. Boivin and S. K. Srivastava, J. Phys. B **31**, 2381 (1998).
[33] R. S. Freund, R. C. Wetzel, R. J. Shul, and T. R. Hayes, Phys. Rev. A **41**, 3575 (1990).
[34] R. G. Montague and M. F. A. Harrison, J. Phys. B **16**, 3045 (1983).
[35] D. S. Belic, R. A. Falk, C. Timmer, and G. H. Dunn, Phys. Rev. A **36**, 1073 (1987).
[36] S. J. T. Hayton and B. Peart, J. Phys. B **27**, 5331 (1994).
[37] M. S. Pindzola, F. Robicheaux, N. R. Badnell, and T. W. Gorczyca, Phys. Rev. A **56**, 1994 (1997).
[38] W. R. Wadt and P. J. Hay, J. Chem. Phys. **82**, 284 (1985).
[39] See http://physics.nist.gov/PhysRefData
[40] D. C. Griffin and M. S. Pindzola, Adv. At., Mol., Opt. Phys. **54**, 203 (2006).
[41] N. R. Badnell, J. Phys. B **30**, 1 (1997).
[42] See http://vanadium.rollins.edu/GASP.html
[43] T. W. Gorczyca and N. R. Badnell, J. Phys. B **30**, 3897 (1997).
[44] D. M. Mitnik, M. S. Pindzola, D. C. Griffin, and N. R. Badnell, J. Phys. B **32**, L479 (1999).
[45] D. M. Mitnik, D. C. Griffin, C. P. Ballance, and N. R. Badnell, J. Phys. B **36**, 717 (2003).
[46] C. P. Ballance and D. C. Griffin, J. Phys. B **37**, 2943 (2004).
[47] For codes, see http://vanadium.rollins.edu/codes
[48] K. A. Berrington, W. B. Eissner, and P. H. Norrington, Comput. Phys. Commun. **92**, 290 (1995).
[49] A. Burgess, J. Phys. B **7**, L364 (1974).
[50] J. M. Rost and T. Pattard, Phys. Rev. A **55**, R5 (1997).
[51] S. M. Younger, Phys. Rev. A **26**, 3177 (1982).
[52] M. S. Pindzola, D. C. Griffin, and C. Bottcher, in *Atomic Processes in Electron-Ion and Ion-Ion Collisions*, NATO Advanced Science Institute B: Physics (Plenum, New York, 1986), Vol. 145, p. 75.
[53] R. D. Cowan, *The Theory of Atomic Structure and Spectra* (University of California Press, Berkeley, 1981).
[54] G. Peach, J. Phys. B **3**, 328 (1970).
[55] E. J. McGuire, Phys. Rev. A **16**, 62 (1977).
[56] L. K. Jha and B. N. Roy, Eur. Phys. J. D **20**, 5 (2002).
[57] F. Karstensen and M. Schneider, J. Phys. B **11**, 167 (1978).
[58] S. Okudaira, Y. Kaneko, and I. Kanomata, J. Phys. Soc. Jpn. **28**, 1536 (1970).
[59] Y. Okuno, K. Okuno, Y. Kaneko, and I. Kanomata, J. Phys. Soc. Jpn. **29**, 164 (1970).
[60] L. A. Vainshtein, V. I. Ochkur, V. I. Rakhovskii, and A. M. Stepanov, Sov. Phys. JETP **34**, 271 (1972).
[61] P. McCallion, M. B. Shah, and H. B. Gilbody, J. Phys. B **25**, 1051 (1992).
[62] E. J. McGuire, Phys. Rev. A **16**, 73 (1977).
[63] S. S. Tayal and R. J. W. Henry, Phys. Rev. A **33**, 3825 (1986).
[64] K. P. Dere, Astron. Astrophys. **466**, 771 (2007).
[65] M. Mattioli, G. Mazzitelli, M. Finkenthal, P. Mazzotta, K. B. Fournier, J. Kaastra, and M. E. Puiatti, J. Phys. B **40**, 3569 (2007).